

Supporting Information For

**Electrochemical quartz crystal microbalance study of covalent
tethering of carboxylated thiol to polyaniline for electrocatalyzed
oxidation of ascorbic acid in neutral aqueous solution**

**Zhaohong Su, Jinhua Huang, Qingji Xie*, Zhengfa Fang, Cong Zhou, Qingmei Zhou,
Shouzhuo Yao**

*Key Laboratory of Chemical Biology and Traditional Chinese Medicine Research (Ministry of
Education of China), College of Chemistry and Chemical Engineering, Hunan Normal
University, Changsha 410081, China*

*To whom correspondence should be addressed. E-mail: xiejq@hunnu.edu.cn. Tel./Fax: +86 731 8865515.

Table 1S The M/n values of PANI–MSA composite films from data shown in **Fig. 6 (B)** and **Fig. 7 (C)** during potential cycling in 0.1 mol L⁻¹ PBS (pH 7.3)^a

film	Q_a ($\times 10^4$ C)	$\Delta f_{0,a}$ (Hz)	$(M/n)_a$ (g mol ⁻¹)	Q_c ($\times 10^4$ C)	$\Delta f_{0,c}$ (Hz)	$(M/n)_c$ (g mol ⁻¹)
PANI _{post} –MSA (P _{a4} /P _{c4})	8.10	-90.0	18.5	11.4	-120	17.6
PANI _{poly} –MSA (P _{a5} /P _{c5})	-7.20	70.0	16.3	-9.20	85.0	15.5

^a Q_a , $\Delta f_{0,a}$ and $(M/n)_a$ as well as Q_c , $\Delta f_{0,c}$ and $(M/n)_c$ denote the oxidation peak charge, frequency shift and M/n of PANI–MSA composite films during potential's positive going as well as the reduction peak charge, frequency shift and M/n of PANI–MSA composite films during potential's negative going. See the text for definitions of other symbols.

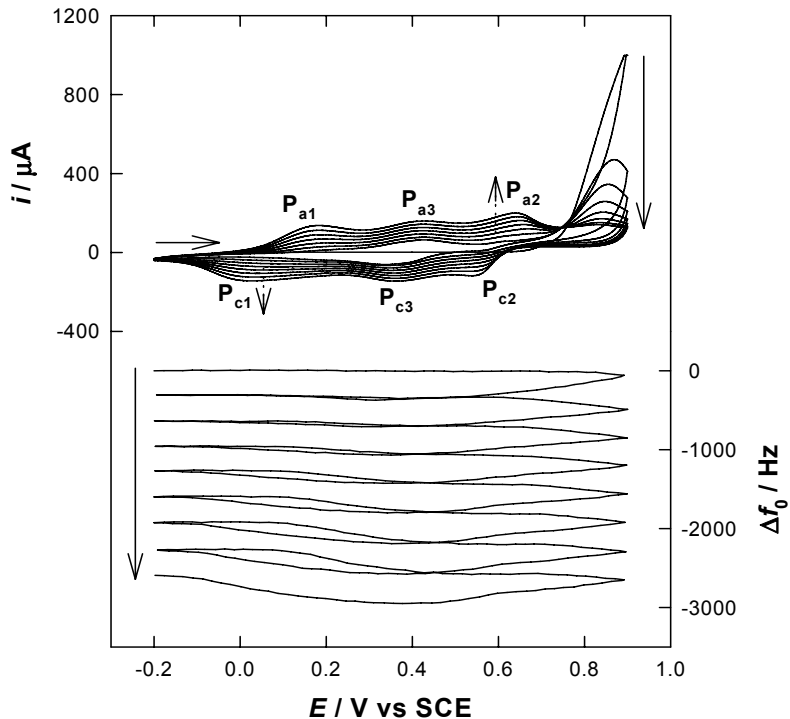


Fig. 1S EQCM responses to cyclic voltammetric polymerization of aniline in 0.1 mol L^{-1} aniline + 0.1 mol L^{-1} H_2SO_4 . Scan rate: 30 mV s^{-1} .

Fig. 1S shows the EQCM responses during the cyclic voltammetric growth of PANI. The aniline monomer was electrooxidized at potentials positive of about 0.79 V vs SCE in the first positive sweep, and the simultaneous frequency decrease demonstrates the onset of polymer deposition on the electrode. Three pairs of redox current peaks, P_{a1}/P_{c1} , P_{a2}/P_{c2} and P_{a3}/P_{c3} , increased cycle by cycle, while the frequency decreased simultaneously, demonstrating that the continuous growth of PANI was taking place. P_{a1}/P_{c1} are attributed to the transition between leucoemeraldine and emeraldine, and P_{a2}/P_{c2} result from the transition between emeraldine and pernigraniline.^{1, 2} P_{a3}/P_{c3} are due to the side reactions of the polymer and oligomers of aniline.³

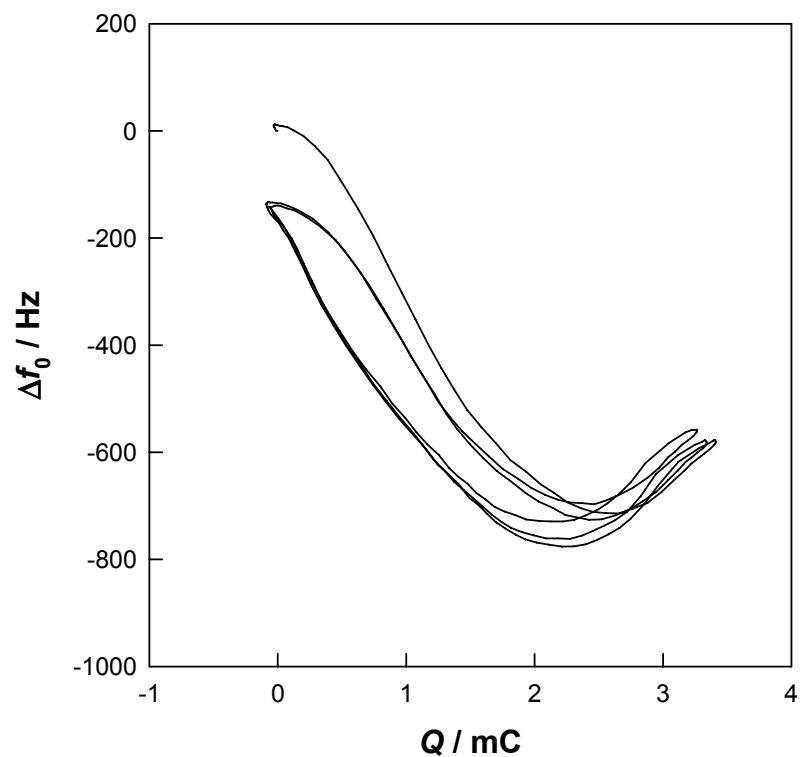


Fig. 2S. Frequency change versus charge curve during potential cycling of a PANI film ($\Delta f_{0,d-PANI} = -2$ kHz) in $0.1\text{ mol L}^{-1}\text{ H}_2\text{SO}_4$ as shown in **Fig. 1 (A)**.

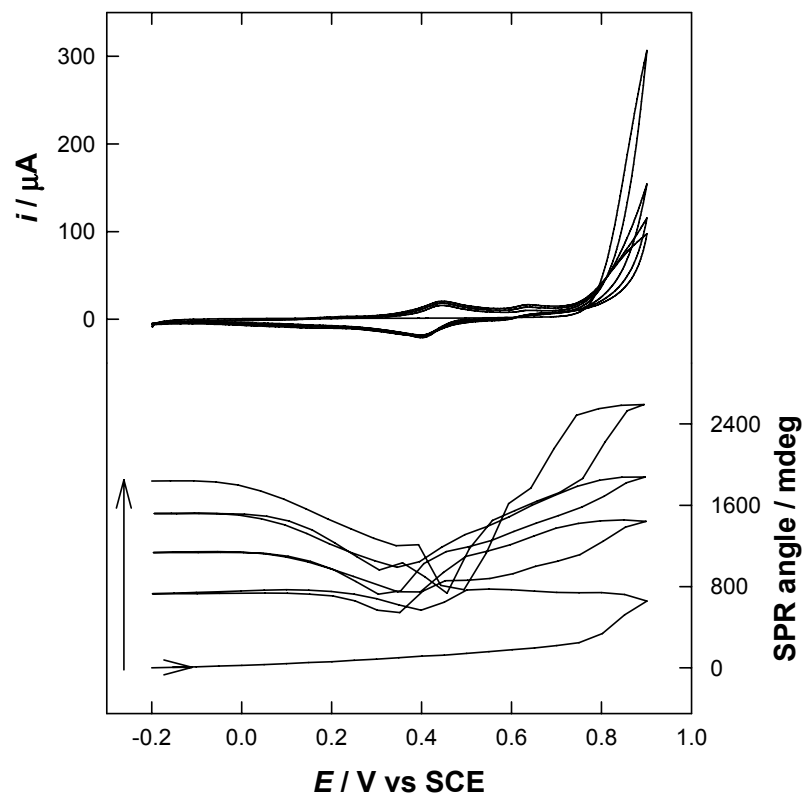


Fig. 3S ESPR responses during aniline electropolymerization in 0.05 mol L^{-1} aniline + 0.1 mol L^{-1} H_2SO_4 . Scan rate: 50 mV s^{-1} . Since the sensitivity of the ESPR response is higher than that of the EQCM frequency response, a PANI film thinner than that for EQCM studies had to be prepared here.

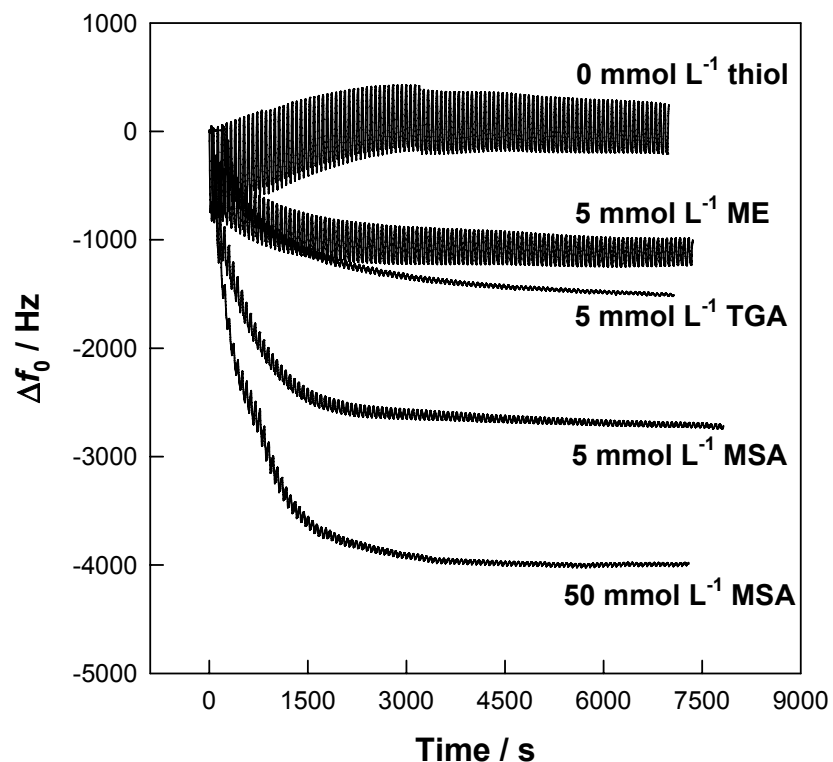


Fig. 4S Time–dependent frequency responses during the interaction of PANI with several thiols.
See **Table 1** in the main text for details.

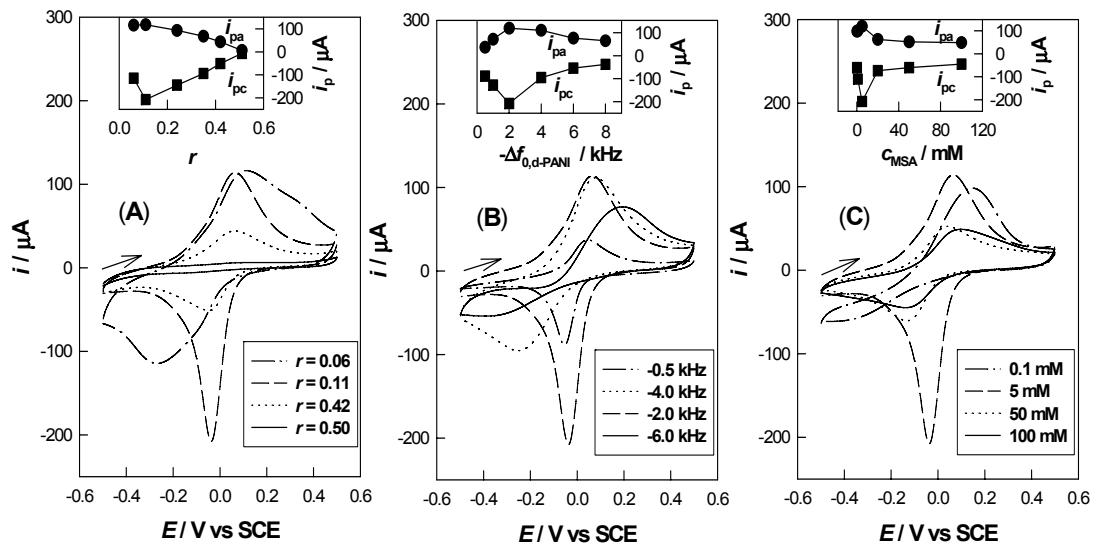


Fig. 5S Cyclic voltammograms (30 mV s^{-1}) for the $\text{PANI}_{\text{post}}\text{-MSA}$ composite films in 0.1 mol L^{-1} PBS ($\text{pH} = 7.3$). Panel A: after interaction of PANI ($\Delta f_{0,d-\text{PANI}} = -2 \text{ kHz}$) with 5 mmol L^{-1} MSA for different potential cycles (1, 3, 10, 20, 50, or 100 cycles at 30 mV s^{-1}) and thus with different r ; panel B: after interaction of -0.5 , -1.0 , -2.0 , -4.0 , -6.0 , or -8.0 kHz PANI ($\Delta f_{0,d-\text{PANI}}$) with 5 mmol L^{-1} MSA for three potential cycles at 30 mV s^{-1} ; and panel C: after interaction of PANI ($\Delta f_{0,d-\text{PANI}} = -2 \text{ kHz}$) with 0.1 , 1 , 5 , 20 , 50 , or 100 mmol L^{-1} MSA for three potential cycles at 30 mV s^{-1} , respectively. Insets show the peak currents as functions of r , the thickness of PANI films and the MSA concentrations, respectively.

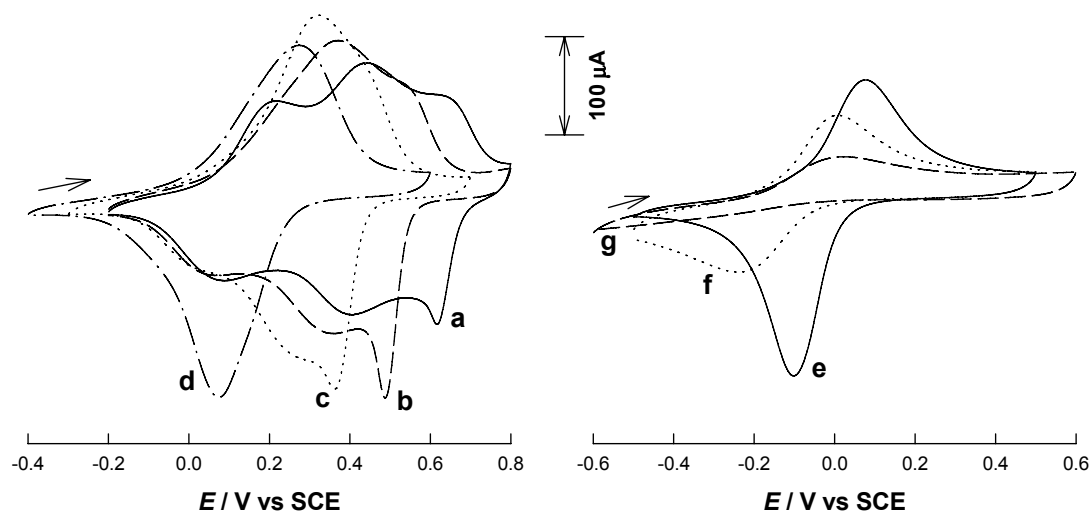


Fig. 6S pH-dependent cyclic voltammograms for a $\text{PANI}_{\text{post}}\text{-MSA}$ composite film ($r = 0.11$) in (a) $0.1 \text{ mol L}^{-1} \text{ H}_2\text{SO}_4$ (pH 0.8) and (b–g) pH 2.0, 3.0, 5.0, 7.0, 8.0 or 9.0 PBS. Scan rate: 30 mV s $^{-1}$.

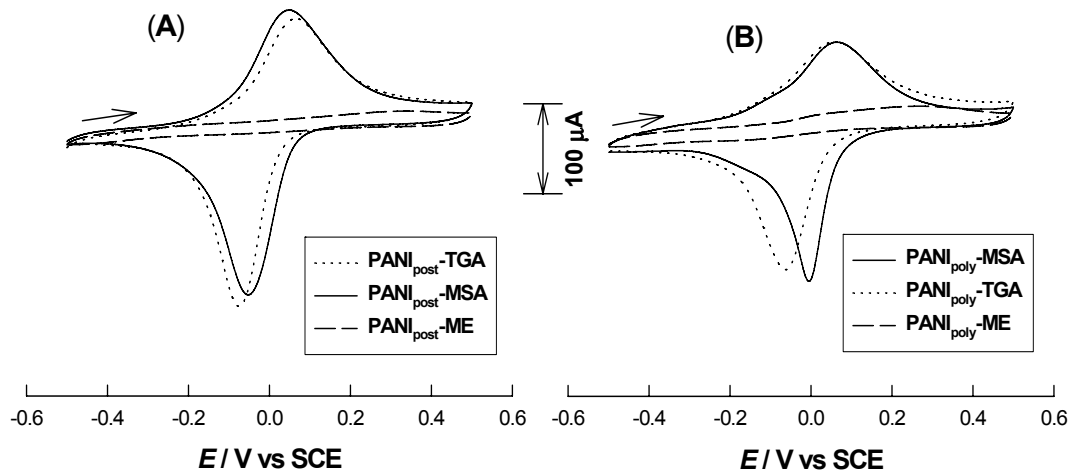


Fig. 7S Cyclic voltammograms for (A) -2.0 kHz PANI_{post}-thiol (5 mmol L^{-1} thiol) composite films and (B) -1.6 kHz PANI_{poly}-thiol composite films obtained from aniline electropolymerization in 0.1 mol L^{-1} aniline + 0.1 mol L^{-1} H₂SO₄ + 0.1 mmol L^{-1} thiol in 0.1 M PBS (pH7.3). Scan rate: 30 mV s^{-1} .

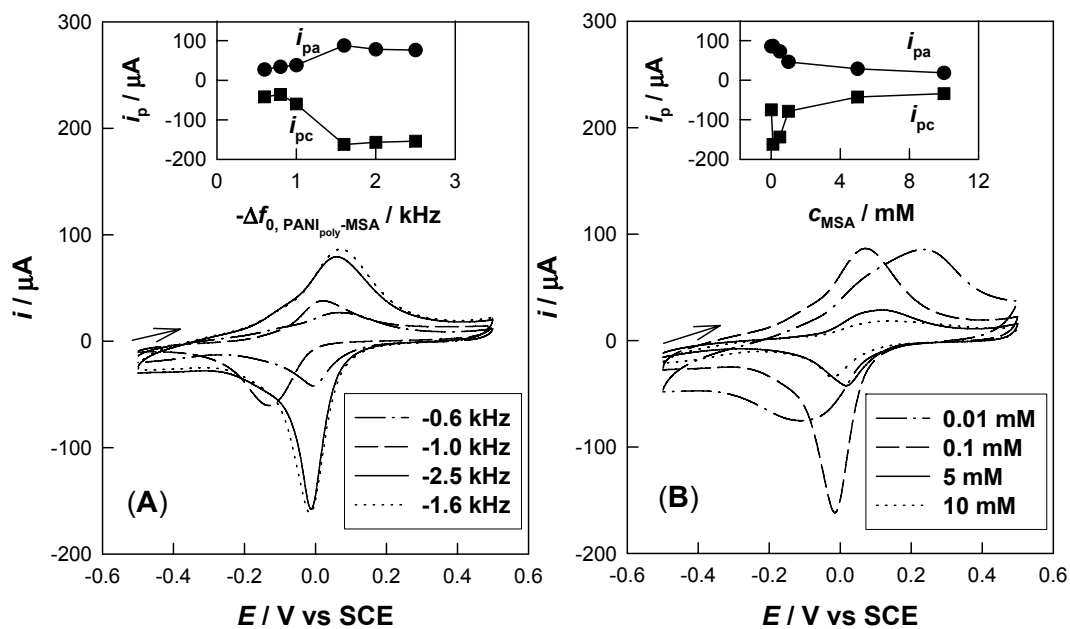


Fig. 8S Cyclic voltammograms (30 mV s^{-1}) for the PANI_{poly}-MSA composite films in 0.1 mol L^{-1} PBS (pH = 7.3). Panel A: for 0.6 , 0.8 , 1.0 , 1.6 , 2.0 , or 2.5 kHz PANI_{poly}-MSA composite films (“wet” frequency), respectively. Panel B: for the PANI_{poly}-MSA composite films obtained from aniline electropolymerization in 0.1 mol L^{-1} aniline + 0.1 mol L^{-1} H₂SO₄ + 0.01 , 0.1 , 0.5 , 1 , 5 , or 10 mmol L^{-1} MSA for 10 potential cycles. Insets show the peak currents as functions of the thickness of PANI_{poly}-MSA films and the concentrations of MSA, respectively.

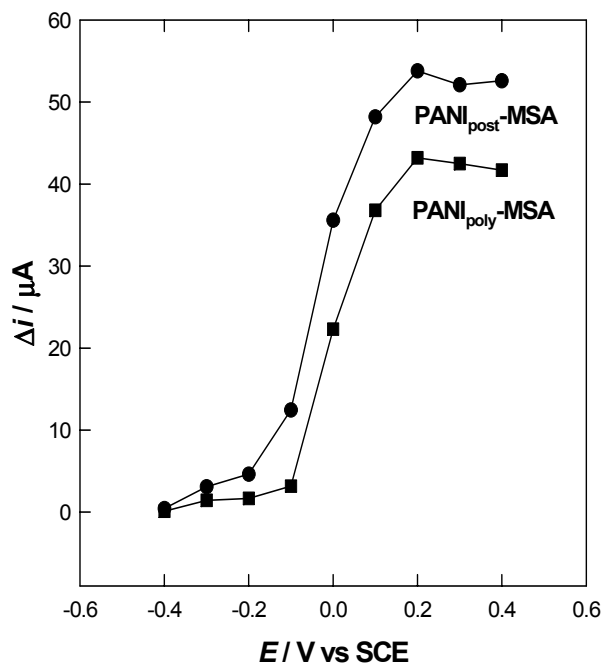


Fig. 9S Effects of the applied potential on the stable current response of the Au electrodes modified with PANI–MSA composite films in 0.1 mol L⁻¹ PBS (pH7.3) containing 1 mmol L⁻¹ AA.

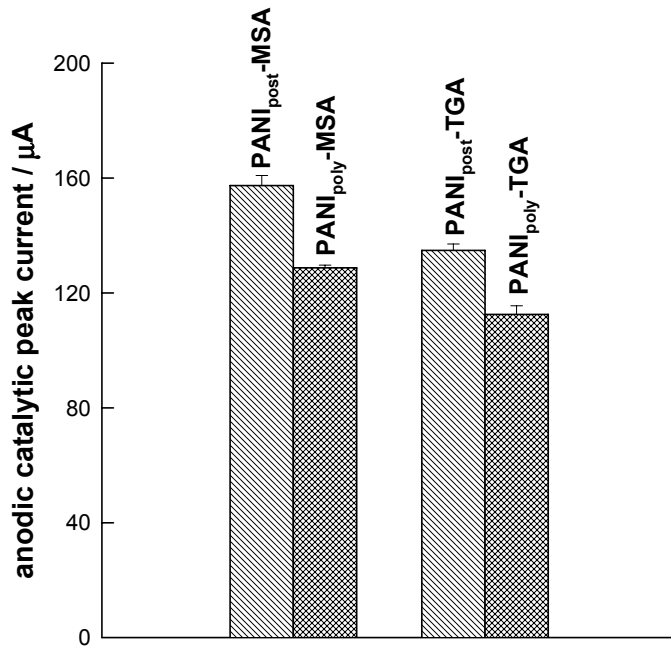


Fig. 10S Anodic catalytic peak currents of $\text{PANI}_{\text{post}}\text{-thiol}$ and $\text{PANI}_{\text{poly}}\text{-thiol}$ measured in 0.1 mol L⁻¹ PBS (pH7.3) in the presence of 1 mmol L⁻¹ AA. Scan rate: 30 mV s⁻¹.

Chronoamperometry was used to investigate the electrode process of AA at the PANI_{post}-MSA/Au electrode. **Fig. 11S** (A) shows the chronoamperometric measurements of AA at various concentrations at the PANI_{post}-MSA/Au electrode at 0.5 V. The Inset of **Fig. 11S** (A) shows the current responses of AA at different concentrations at fixed times of 4, 10 and 16 s, respectively. It can be seen from the plots that the slopes of the calibrations decrease with increasing time after the potential step application. However, there is a very similar intersection between currents measured at different time elapsed and AA concentrations. The typical $I-t$ curve in **Fig. 11S** (A) indicates that the currents observed must be controlled by AA diffusion in solution. Thus, the current corresponding to the electrochemical reaction obeys Cottrell's law,⁴

$$I = nFAD^{1/2}c_0/\pi^{1/2}t^{1/2} \quad (1)$$

where D and c_0 are the diffusion coefficient ($\text{cm}^2 \text{ s}^{-1}$) and bulk concentration (mol cm^{-3}), respectively. Based on Eq. (1) the plot of I versus $t^{1/2}$ is a straight line, and the slope of such lines can be used to estimate the diffusion coefficient of AA. The mean value of D is found to be $8.3 \times 10^{-6} \text{ cm}^2 \text{ s}^{-1}$, which is in good agreement with that obtained from the rotating disk electrode (RDE) voltammetry technique.^{5,6}

Chronoamperometry can also be employed to evaluate the catalytic rate constant for the reaction between AA and the redox sites of the surface confined PANI-thiol film according to the method of Galus⁷:

$$I_{\text{cat}}/I_l = \gamma^{1/2}[\pi^{1/2}\text{erf}(\gamma^{1/2}) + \exp(-\gamma)/\gamma^{1/2}] \quad (2)$$

where I_{cat} is the catalytic current of AA at the PANI_{post}-MSA/Au electrode, I_l is the limiting current in the absence of AA, and $\gamma = kc_0t$ (c_0 is the bulk concentration of AA). When γ

exceeds 2, the error function is almost equal to 1 and therefore the above equation can be reduced to

$$I_{\text{cat}}/I_l = \gamma^{1/2} \pi^{1/2} = \pi^{1/2} (kc_0 t)^{1/2} \quad (3)$$

where t is the time elapsed (s). Based on the slope of the I_{cat}/I_l versus $t^{1/2}$ plot, k can be obtained for a given AA concentration. One such plot is shown in **Fig. 11S (B)** constructed from the chronoamperogram of the PANI_{post}-MSA/Au electrode in the absence and presence of 2 mmol L⁻¹ AA. The mean value of k in an AA concentration range of 0.5–5 mmol L⁻¹ was obtained to be 7.2×10^5 cm³ mol⁻¹ s⁻¹. This result is close to those obtained from RDE voltammetry.^{5, 6} Under the same conditions, the k for PANI_{poly}-MSA/Au electrode was similarly obtained to be 2.7×10^5 cm³ mol⁻¹ s⁻¹. The obtained k values agree well with the reported value from chronoamperometry for PANI doped with camphorsulfonic acid (5.6×10^5 cm³ mol⁻¹ s⁻¹) or β -naphthalenesulfonic acid (6.2×10^5 cm³ mol⁻¹ s⁻¹).^{5, 6}

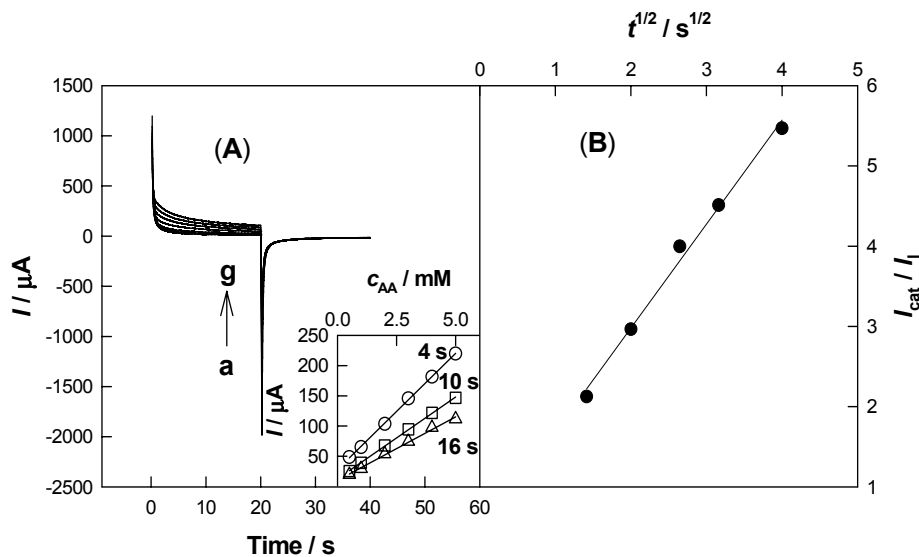


Fig. 11S (A) Chronoamperograms obtained in 0.1 mol L⁻¹ PBS (pH 7.3) at the PANI_{post}-MSA/Au ($r = 0.11$) electrode in the absence (a) and presence of 0.5 (b), 1 (c), 2 (d), 3 (e), 4 (f) or 5 (g) mmol L⁻¹ AA. The first and second potential steps were 0.5 and -0.5 V, respectively. Inset shows the dependence of the fixed-time current (observed at 4, 10 and 16 s after the first potential step) versus AA concentration. (B) Dependence of I_{cat}/I_l on $t^{1/2}$ derived from the data of chronoamperograms of (a) and (d) in **Fig. 11S (A)**.

References

- 1 D. Orata, D. A. Buttry, *J. Am. Chem. Soc.*, 1987, **109**, 3574.
- 2 B. C. Sherman, W. B. Euler, R. R. Forcé, *J. Chem. Educ.*, 1994, **71**, A94.
- 3 E. M. Geniès, M. Lapkowski, J. F. Penneau, *J. Electroanal. Chem.*, 1988, **249**, 97.
- 4 A. J. Bard, L. R. Faulkner, *Electrochemical methods, Fundamentals and Applications*, Wiley, New York, 1980.
- 5 L. Zhang, *Electrochim. Acta*, 2007, **52**, 6969.
- 6 L. Zhang, S. Dong, *J. Electroanal. Chem.*, 2004, **568**, 189.
- 7 Z. Galus, *Fundamentals of Electrochemical Analysis*, Ellis Horwood Press, New York, 1976.